



CORROSION STUDIES ON GAS TUNGSTEN ARC SURFACE MELTED AZ91C MAGNESIUM ALLOY

C. Padmavathi, K. Srinivasa Rao, K. Prasad Rao

*Department of Metallurgical and Materials Engineering
Indian Institute of Technology Madras, Chennai – 600 036*

ABSTRACT

AZ91C magnesium alloy castings exhibit poor corrosion resistance due to coarser grains and segregation of magnesium and aluminum to grain boundaries. In this work, surface melting of the cast material by gas tungsten arc technique (GTAW) was done to refine grain size and also to reduce the segregation. Corrosion behavior was studied in 3.5% NaCl solution by electrochemical method. The corrosion behavior was related to microstructural changes produced during the surface melting process. The results showed that GTAW surface melting helps to improve corrosion resistance of cast AZ91C alloy.

Keywords: AZ91C, GTAW, surface melting, corrosion.

1. INTRODUCTION

The corrosion resistance of the cast Magnesium-Aluminum alloys depends considerably on microstructure and the environment to which it is exposed [1]. The microstructure of cast AZ91C magnesium alloy consists of eutectic mixture of $Mg_{17}Al_{12}$ intermetallic phase and α - Mg matrix. The intermetallic compounds significantly reduce the corrosion resistance because of large corrosion potential difference between the intermetallic compounds and the magnesium matrix [2]. The $Mg_{17}Al_{12}$ phase is a principal precipitate in the Mg-Al alloy system, resulting from the high aluminum content [3]. It is assumed that gas tungsten arc surface melting technique resulted in grain refinement and finer microstructure $Mg_{17}Al_{12}$ that in turn improved corrosion resistance of AZ91C cast alloy. Electrochemical properties for the cast AZ91C alloy were studied by polarization behavior.

2. EXPERIMENTAL PROCEDURE

Die cast plates of AZ91C magnesium alloy were used as target for surface melting by GTAW process. The chemical composition of AZ91C alloy was determined by optical emission spectroscopy is shown in Table-1. Surface melting was carried out with an alternating current (AC) polarity gas tungsten arc machine with continuous arc current (CC) and pulsed arc current (PC) mode. Table-2 & 3 shows the parameters used for the surface melting process. A continuous flow of high purity argon gas protected the surface of the specimens during surface melting process. Optical microstructural observations and phase analysis (by X-Ray diffraction method) were carried out before and after gas tungsten arc surface melting.

Electrochemical polarization experiments were carried out in a corrosion cell containing 150ml of 3.5% NaCl solution using a standard three-electrode configuration. A standard calomel electrode (SCE) was used as a reference electrode and graphite electrode was used as counter electrode and testing area regulated to 100mm². Polarization scanning was carried out from – 1900mV to – 400mV (SCE) at a scan rate of 0.5mV/S to construct the tafel plots (logarithmic

variation of current as function of voltage. The corrosion current was determined from the intersection of these two linear plots [4]. The corrosion behavior was investigated by a detailed microstructural observation and phase analysis (X-Ray diffraction method) of corroded film on surface melted and cast AZ91C alloy.

3. RESULTS AND DISCUSSION

3.1 Microstructures

3.1.1 Cast AZ91C magnesium alloy

Figure-1 showed the aluminum-magnesium phase diagram. The microstructure consists of eutectic mixture of matrix of α - Mg grains with the β phase (intermetallic $Mg_{17}Al_{12}$) along the α grain boundaries as shown in figures 2a and 2b. From the microstructure of the cast AZ91C magnesium alloy; it is evident that the aluminum is partly in solid solution and partly precipitated along grain boundaries as a continuous phase as well as part of lamellar structure.

3.1.2 Gas tungsten arc surface melted AZ91C alloy

Gas tungsten arc surface melted alloy produced a defect free microstructure with the pronounced grain refinement with both continuous and pulsed arc current mode technique, which is evident from figures 4a and 5a. The depth of melting in gas tungsten arc surface melted was found to be 500 μ m. The substrate grains were significantly coarser than the surface melted alloy. The $Mg_{17}Al_{12}$ morphology of melted alloy was found to be significantly refined and redistributed along the grain boundaries. Almost continuous and continuous $Mg_{17}Al_{12}$ precipitation was observed for continuous and pulsed arc current mode as shown in figures 4b & 5b.

3.2 Microhardness study

The microhardness of surface melted alloy significantly increased in the range of 84VHN to 111VHN after GTAW melting as compared to cast alloy (74 VHN). This improvement in microhardness may be attributed due to the grain refinement. Enhancement in microhardness with refined microstructure is expected to improve the wear resistance of AZ91C magnesium alloy.

3.3 X-Ray diffraction Analysis

The surface of the cast alloy showed mainly peaks corresponding to Mg and β phase as shown in figure-3. The X-Ray diffraction pattern showed the presence of both the phases α and β in surface melted samples, for both continuous and pulsed arc current mode. The peaks corresponding to β phase were more intense for surface melted alloy as compared to that of die cast alloy, which is shown in figure-6.

3.4 Electrochemical study

The table-4 shows the E_{corr} , I_{corr} values of cast and surface melted alloy. Gas tungsten arc surface melted alloy showed better corrosion resistance as result of surface melting. For example cast alloy showed E_{corr} value of -1534mV whereas it becomes positive by surface melting which is evident from figure-7. The I_{corr} values were found to decrease after surface melting. These results show that GTAW surface melting is beneficial in improving corrosion resistance of cast AZ91C.

3.5 Characterization of corroded AZ91C magnesium alloy

3.5.1 Microstructure of corroded AZ91C alloy

The corrosion morphology shows that the surface of the as-cast specimen was corroded severely compared to as of the surface melted specimens as shown in figures 8a, 9a, and 10a. The matrix α phase in the magnesium alloys is normally anodic to intermetallic phase $Mg_{17}Al_{12}$, with the result α phase is usually preferentially corroded as shown in figures-8b, 9b & 10b. The corrosion of α - matrix was activated because of the decrease in aluminum content resulting from β precipitation (discontinuous). In the cast AZ91C alloy, the primary and eutectic α phase forms a galvanic corrosion cells with β phase. Surface melting which resulted in finer structure was helpful in reducing the corrosion rate of the surface.

Corrosion attack on the surface melted alloy was decreased which may attributed due to the following reasons,

1. Smaller the grains, higher the grain boundaries areas, therefore more precipitates and thereby decreased the anode and cathode area ratio due to the significant grain refinement and $Mg_{17}Al_{12}$ precipitate redistribution along the grain boundaries.
2. The β precipitation formed an almost continuous β phase barrier along the grain boundaries, which suppressed the development of corrosion.
3. The grain boundaries have a high level of aluminum in solid solution [5] and in general have higher corrosion resistance than the lower aluminum grain interior.
4. Further, higher aluminum content adjacent to the β phase reduces the corrosion rate of AZ91C magnesium alloy.
5. Thus $Mg_{17}Al_{12}$ phase served as effective barrier and suppressed the further propagation of the corrosion.

3.5.2 X-Ray diffraction Analysis

Figures 11 & 12 showed the X-Ray diffraction pattern of the corroded scale formed on as received cast and surface melted specimens. It is evident that the surface scale of both specimens consisted of $Mg(OH)_2$ along the peaks of the Mg . The $Mg(OH)_2$ film on the surface melted samples was more stable because of the finer grain size of the matrix underneath, whereas in the case of as-received cast alloy, the hydroxide film was less stable and easily dissolved in the presence of chloride ions [6].

4.0 CONCLUSIONS

In these investigations, it is clear that the Gas tungsten arc surface melting is capable of improving significantly the resistance to corrosion of cast AZ91C magnesium alloy. It also improved the microhardness.

1. Gas tungsten surface melting resulted in significant improvement in the corrosion resistance of the AZ91C alloy, which can be attributed to the grain refinement and fine grain boundary precipitates.
2. The corrosion potential increased from -1534mV to -1402mV as a result of surface melting for AZ91C alloy.
3. Surface melting increased the microhardness from 74 VHN (cast) to 111 VHN (GTAW melted) of AZ91C magnesium alloy.

4. XRD analysis showed that the microstructural constituents are nearly identical in as cast and gas tungsten arc surface melted specimens and also showed the more intense peaks corresponding to $Mg_{17}Al_{12}$ in surface melted AZ91C alloy.
5. Microstructure of surface melted alloy showed that the pronounced grain refinement and redistribution of the intermetallic phase $Mg_{17}Al_{12}$.
6. Gas tungsten arc melting can be used in actual practice to improve corrosion resistance of AZ91C alloy.

REFERENCES

1. Rajan Ambat*, Naing Naing Aung, W.Zhou, *Corro. Sc.* 42(2000) p 1433.
2. Yong-iin Ko, Chang Dong Yim, Jong Dae Lim and Kwang Seon Shin, *Mater. Sc. forum vols.* 419-422(2003) p 851.
3. M.G.Fontana (Ed). *Corro. Eng.* (1987), p 71.
4. G.Song, A.Atrens, M.Dargush, *Corro. Sc.*, 41 (1999), p 249.
5. E.Aghion, B.Bronfin, in: G: W Lorimer (Ed), *Proceedings of the third international magnesium conference*, Manchester, (1996), p 313.
6. E.Mc caffey, P.Moore, *J.Electro. Soci.* 133(1986) p 1090.

TABLES

Table-1

Mg	Al	Zn	Mn	Si	Cu	Ni
Remainder	8.8	0.68	0.22	0.20	0.08	0.01

Table-2

AC Techniques (pulsed current)	Current A		Voltage V	Travel Speed (mm/min)	Frequency (Hz)
	Base	Peak			
PC	30	70	18	300	6

Table-3

Continuous current	Current A	Voltage V	Travel speed (mm/min)
CC	50	16	300

Table-4

Corrosion parameters	Base metal	TIG PC	TIG CC
Ecorr values (mV)	-1534	-1423	-1402
Icorr values (mA)	1.211	0.09301	0.0697

FIGURES

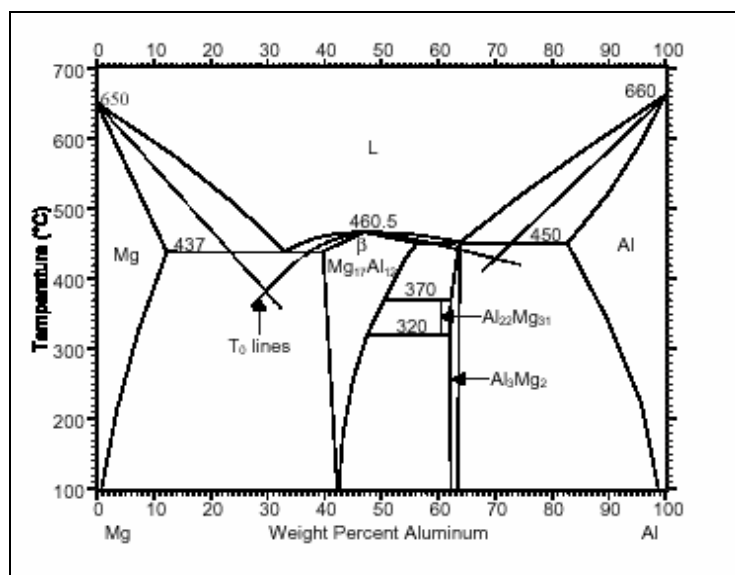


Fig-1 Al-Mg phase diagram.

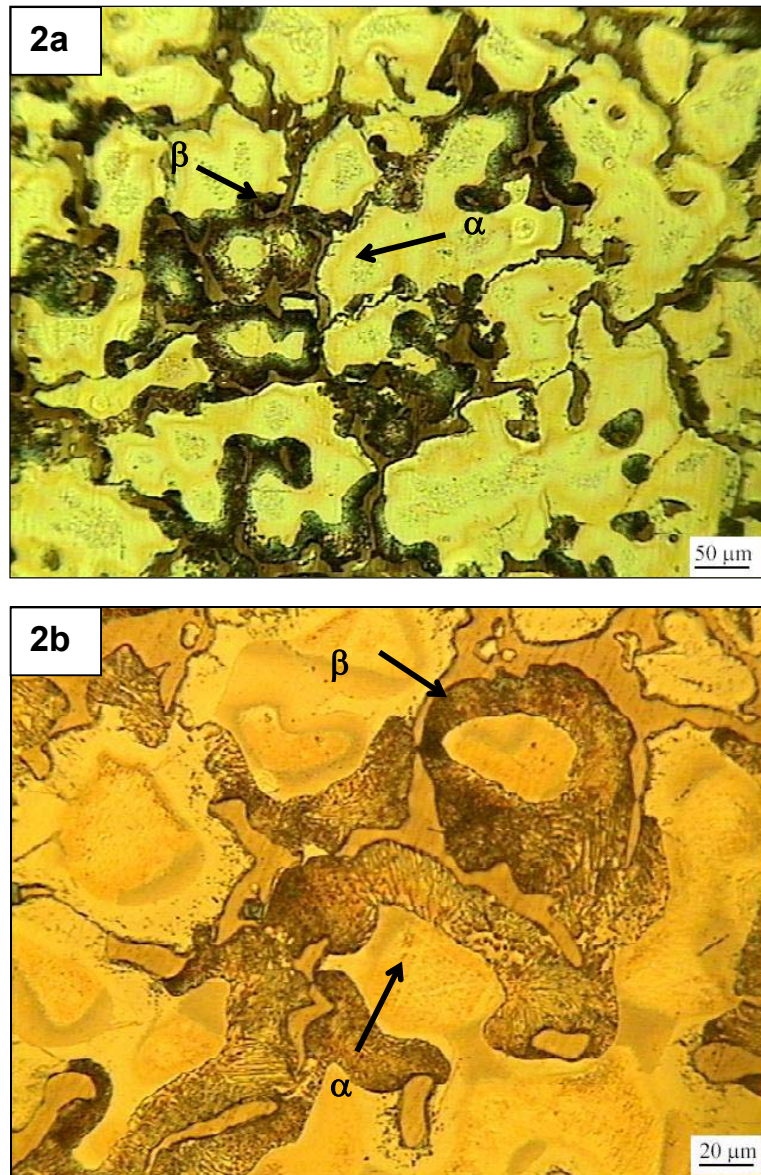


Fig-2a & 2b, Microstructures of cast AZ91C alloy.

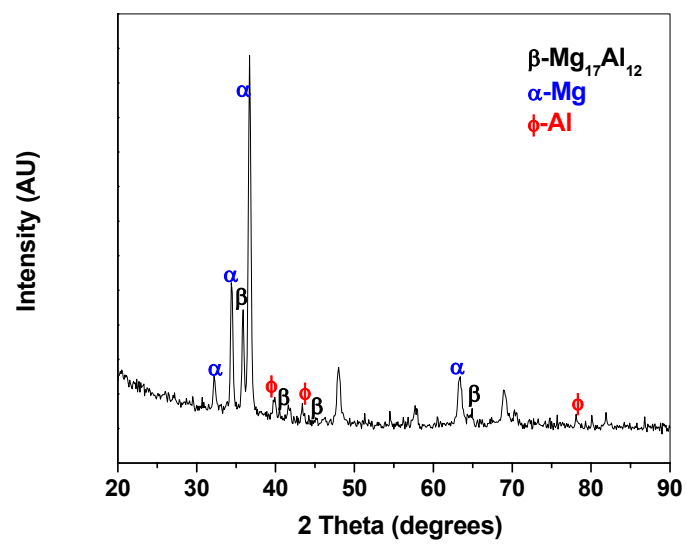


Fig-3 XRD pattern for Cast AZ91C magnesium alloy.

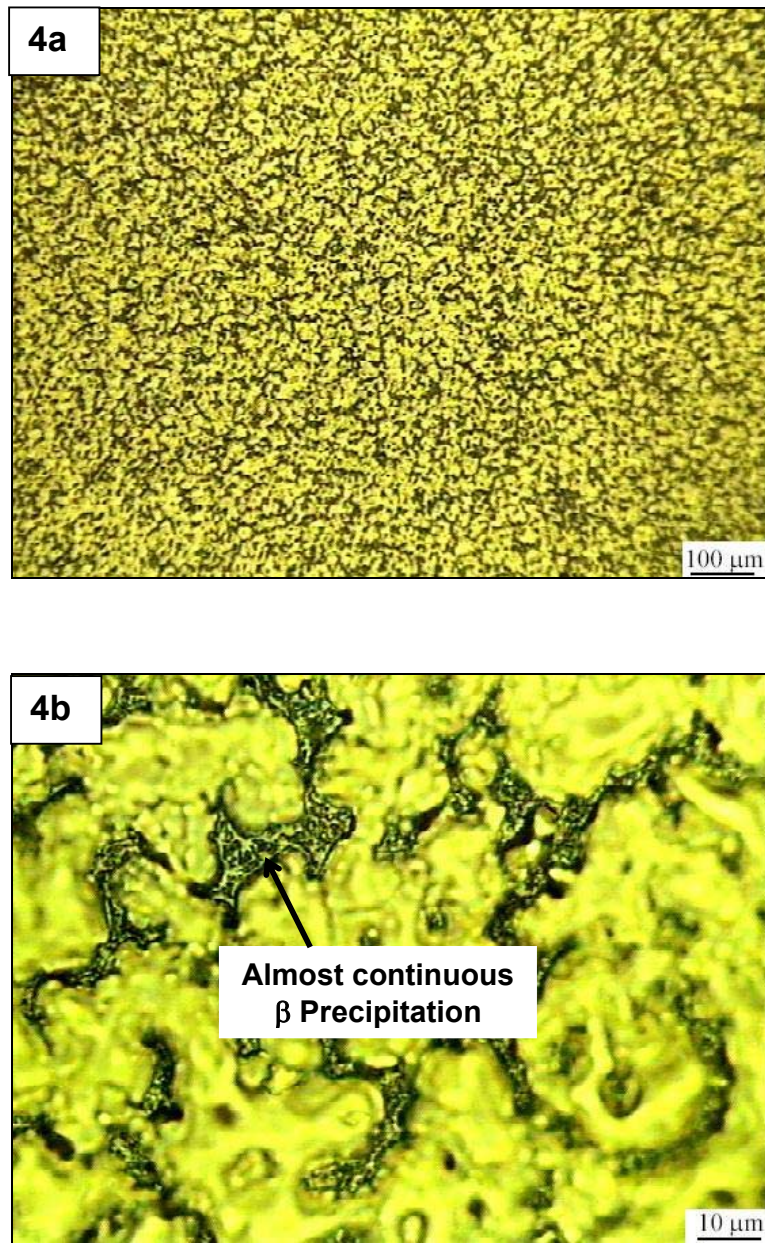


Fig-4a & 4b Microstructures of surface melted AZ91C alloy (continuous current).

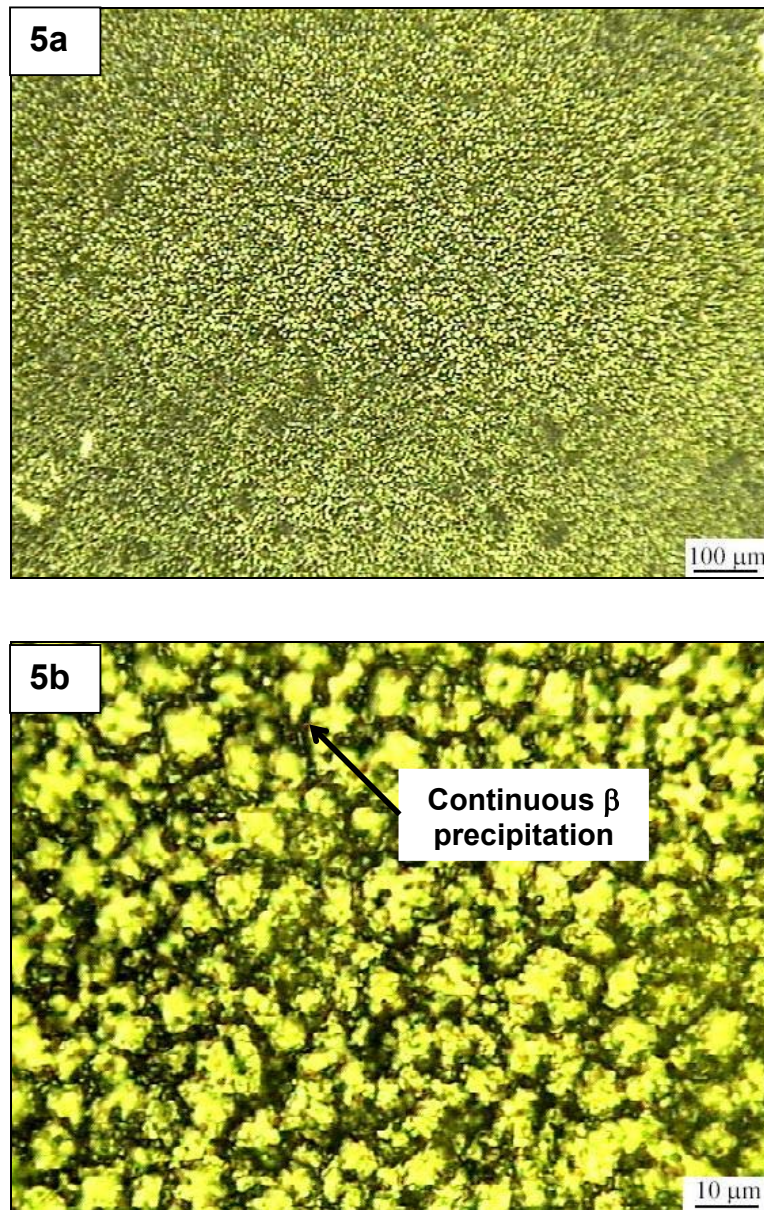


Fig-5a & 5b, Microstructures of surface melted AZ91C alloy (pulsed current).

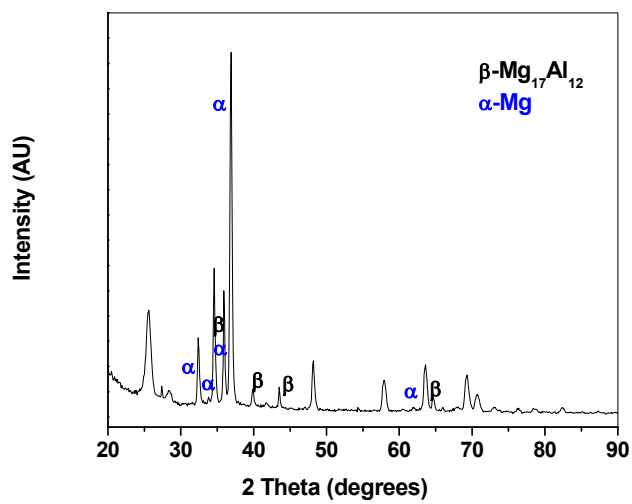


Fig-6 Typical XRD pattern for surface melted AZ91C alloy

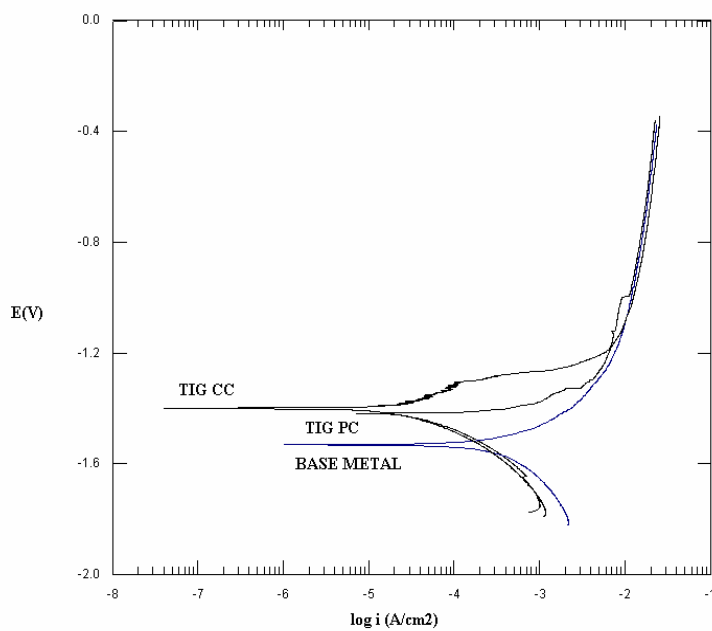


Fig-7 Polarization curves for cast and surface melted AZ91C alloy in 3.5% NaCl solution.

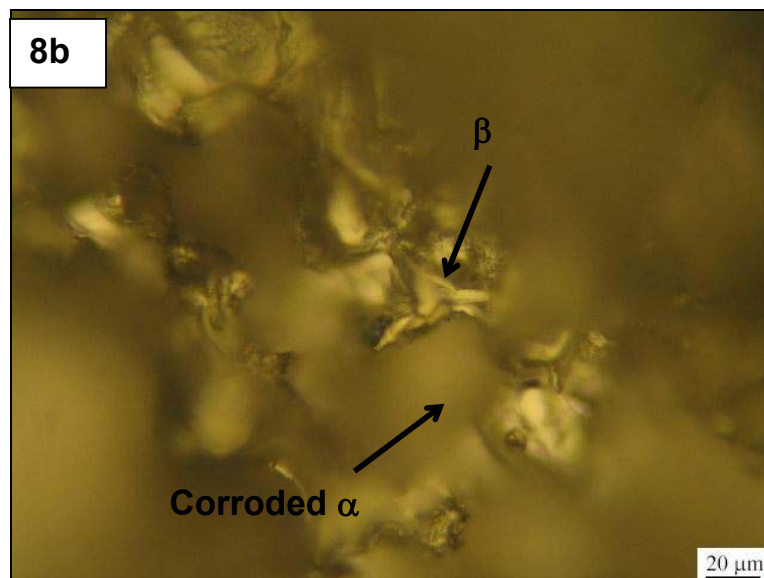


Fig-8a & 8b, Microstructures of corroded base metal AZ91C alloy

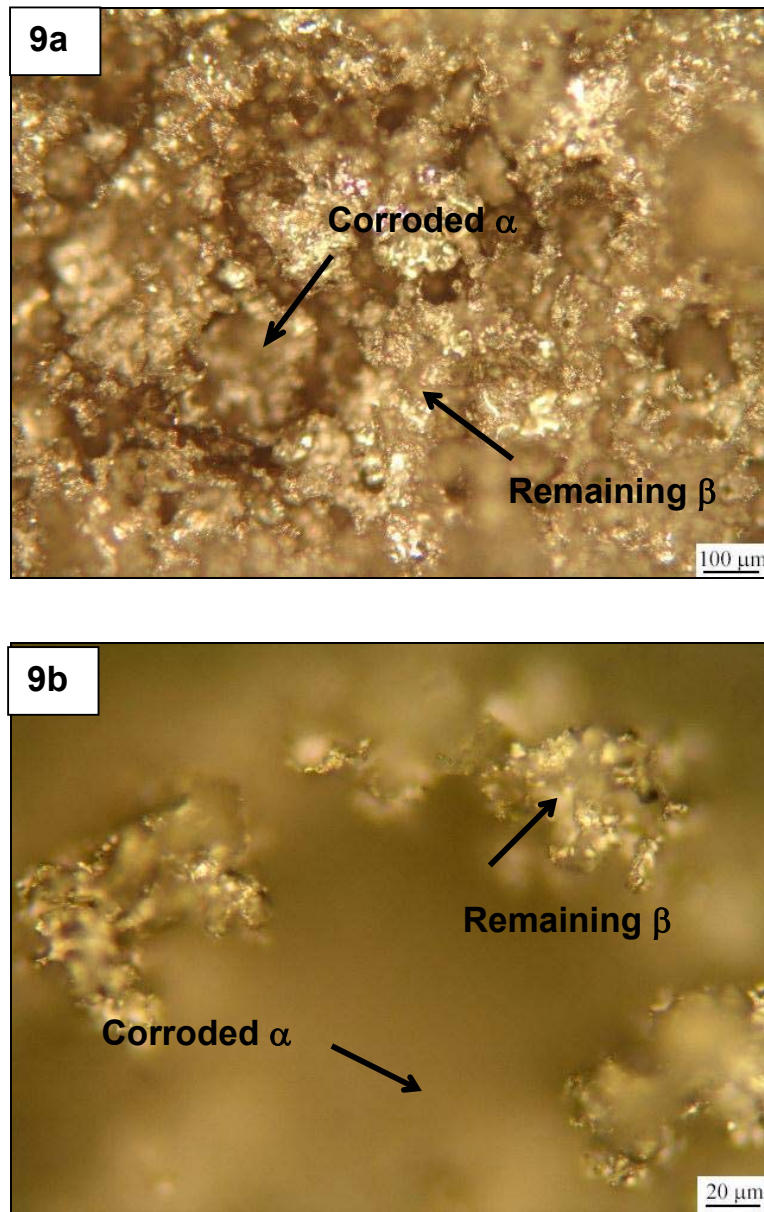


Fig-9a & 9b Microstructures of corroded surface melted alloy (Continuous current).

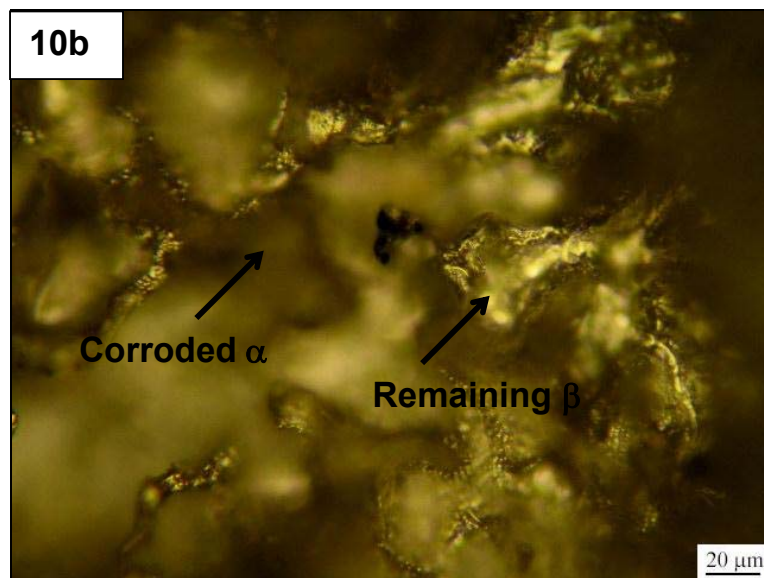
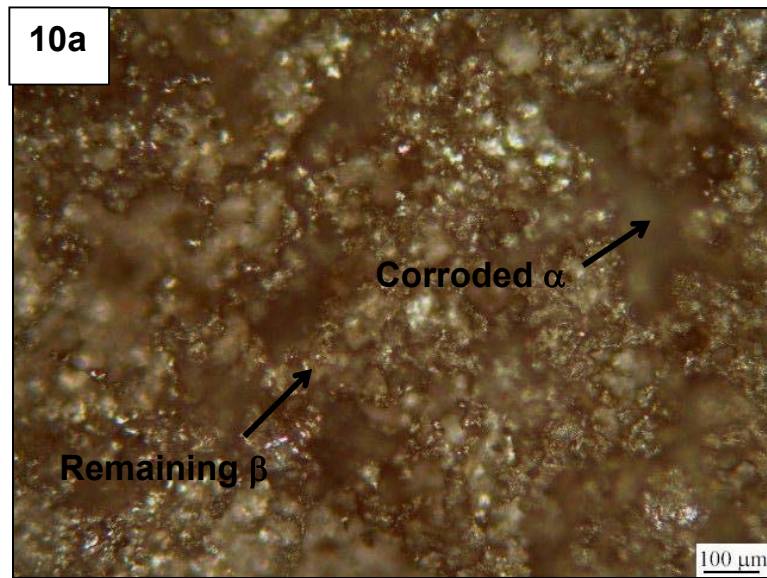


Fig-10a & 10b Microstructures of corroded surface melted alloy (Pulsed current).

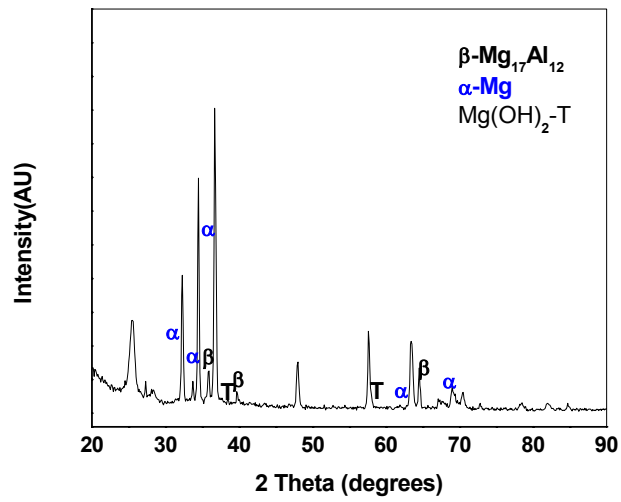


Fig-11 Typical XRD pattern for corroded cast AZ91C alloy.

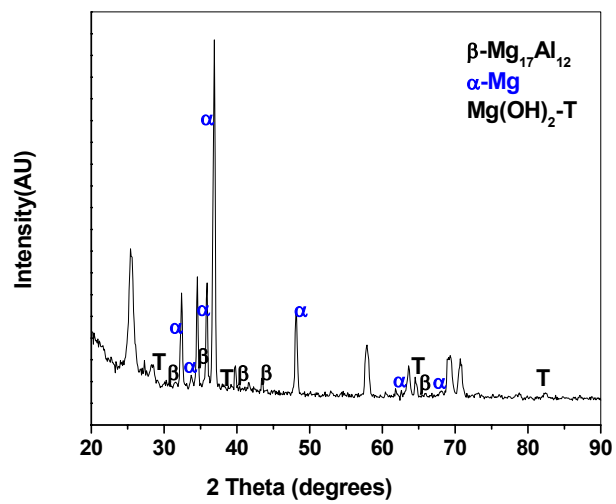


Fig-12 Typical XRD pattern for corroded surface melted alloy.